JNeurosci
THE JOURNAL OF NEUROSCIENCE

Research Articles: Systems/Circuits

Astrocytes modulate baroreflex sensitivity at the level of the nucleus of the solitary tract

https://doi.org/10.1523/JNEUROSCI.1438-19.2020

Cite as: J. Neurosci 2020; 10.1523/JNEUROSCI.1438-19.2020

Received: 4 August 2019
Revised: 16 December 2019
Accepted: 12 January 2020

Astrocytes modulate baroreflex sensitivity at the level of the nucleus of the solitary tract

Svetlana Mastitskaya[1], Egor Turovsky[2], Nephtali Marina[1], Shefeeq M. Theparambil[1], Anna Hadjihambi[1], Sergey Kasparov[3,4], Anja G. Teschemacher[3], Andrew G. Ramage[1], Alexander V. Gourine[1*] and Patrick S. Hosford[1,5*]

[1]Centre for Cardiovascular and Metabolic Neuroscience, Department of Neuroscience, Physiology and Pharmacology, University College London, London WC1E 6BT, United Kingdom.

[2]Institute of Cell Biophysics, Russian Academy of Sciences, Pushchino, 142290, Russian Federation.

[3]Physiology, Pharmacology and Neuroscience, University of Bristol, BS8 1TD, United Kingdom

[4]Baltic Federal University, Kaliningrad, 236041, Russian Federation.

[5]William Harvey Research Institute, Barts and The London School of Medicine and Dentistry, London EC1M 6BQ, United Kingdom.

*Corresponding authors:
AVG; a.gourine@ucl.ac.uk,
PSH; p.hosford@qmul.ac.uk

Abstract

Maintenance of cardiorespiratory homeostasis depends on autonomic reflexes controlled by neuronal circuits of the brainstem. The neurophysiology and neuroanatomy of these reflex pathways are well understood, however, the mechanisms and functional significance of autonomic circuit modulation by glial cells remain largely unknown. In experiments conducted in male laboratory rats we show that astrocytes of the nucleus tractus solitarii (NTS), the brain area that receives and integrates sensory information from the heart and blood vessels, respond to incoming afferent inputs with $[Ca^{2+}]_i$ elevations. Astroglial $[Ca^{2+}]_i$ responses are triggered by transmitters released by vagal afferents, glutamate acting at AMPA receptors and 5-HT acting at 5-HT_{2A} receptors. In conscious freely behaving animals blockade of Ca^{2+}-dependent vesicular mechanisms in NTS astrocytes by virally driven expression of a dominant-negative SNARE protein (dnSNARE) increased baroreflex sensitivity by 70% ($p<0.001$). The effect of compromised astroglial function was specific to the NTS as expression of dnSNARE in astrocytes of the ventrolateral brainstem had no

effect. ATP considered the principle gliotransmitter and is released by vesicular mechanisms affected by dnSNARE expression. Consistent with this hypothesis, in anesthetized rats, activation $P2Y_1$ purinoceptors in the NTS decreased baroreflex gain by 40% ($p=0.031$), while blockade of $P2Y_1$ receptors increased baroreflex gain by 57% ($p=0.018$). These results suggest that glutamate and 5-HT released by NTS afferent terminals trigger Ca^{2+}-dependent astroglial release of ATP to modulate baroreflex sensitivity via $P2Y_1$ receptors. These data add to the growing body of evidence supporting an active role of astrocytes in the brain information processing.

Significance statement

Cardiorespiratory reflexes maintain autonomic balance and ensure cardiovascular health. Impaired baroreflex may contribute to the development of cardiovascular disease and serves as a robust predictor of cardiovascular and all-cause mortality. The data obtained in this study suggest that astrocytes are integral components of the brainstem mechanisms that process afferent information and modulate baroreflex sensitivity via the release of ATP. Any condition associated with higher levels of 'ambient' ATP in the NTS would be expected to decrease baroreflex gain by the mechanism described here. As ATP is the primary signalling molecule of glial cells (astrocytes, microglia) responding to metabolic stress and inflammatory stimuli, our study suggests a plausible mechanism of how the central component of baroreflex is affected in pathological conditions.

Introduction

Operation of all fundamental reflexes essential for the maintenance of cardiorespiratory homeostasis is controlled by the autonomic circuits located in the lower brainstem. Cardiorespiratory reflexes ensure autonomic balance and maintain cardiovascular health. Impaired operation of these reflexes (the baroreflex in particular) may contribute to the development of cardiovascular disease and serves as a robust predictor of cardiovascular and all-cause mortality (La Rovere et al., 1998; La Rovere et al., 2001; McCrory et al., 2016). Brainstem autonomic circuits receive sensory information via afferent fibers running within the IX^{th} (glossopharyngeal) and X^{th} (vagus) cranial nerves. These

afferents terminate in the nucleus of the solitary tract (NTS), located in the dorsal aspect of the brainstem, and release glutamate as the principal transmitter at the first central synapse (Talman, 1997; Baude et al., 2009).

Glutamatergic transmission (essential for the processing of afferent information) in the NTS is modulated by other transmitter systems (see Sevoz-Couche and Brouillard, 2017), with 5-hydroxytryptamine (serotonin, 5-HT) playing a key role (Ramage and Villalón, 2008; Hosford and Ramage, 2019). The transmitters and receptors involved in signal processing in the NTS have been extensively studied. However, the role of astrocytes in this brain area is less well understood. This is despite a notable abundance and complexity of the NTS astrocytes (Dallaporta et al., 2010; SheikhBahaei et al., 2018a) and significant evidence that astrocytes modulate the activities of many other CNS circuits, - for example, these involved in learning and memory (Han et al., 2012; Navarrete et al., 2012), control of sleep (Halassa et al., 2009) and regulation of breathing (Gourine et al., 2010; Sheikhbahaei et al., 2018b).

Two previous studies suggested a potentially important role of astrocytes in the mechanisms underlying processing of cardiovascular sensory information in the NTS. McDougal and colleagues reported that electrical stimulation of the solitary tract in a brainstem slice preparation activates the NTS astrocytes (shown by an increase in $[Ca^{2+}]_i$) via the mechanism involving AMPA receptors (McDougal et al., 2011). Lin and colleagues demonstrated that ablation of NTS astrocytes (using the ribosomal toxin saporin) impairs baroreflex sensitivity, alters chemo- and von Bezold-Jarisch reflexes, leading to profound blood pressure lability and, in some animals, sudden cardiac death (Lin et al., 2013). Together, these findings indicate that NTS astrocytes can respond to vagal input and may play an important role in the control of cardiovascular reflexes. However, physical ablation of astrocytes removes the structural and metabolic support they provide to neurons and thus could mask the subtleties of their role in transmission and integration of cardiovascular afferent information by the NTS circuits. Therefore, it remains unknown how NTS astrocytes are recruited by vagal afferent input and the importance of astroglial signalling for the operation of the cardiovascular reflexes.

In the present study we addressed these questions by performing *in vivo* $[Ca^{2+}]_i$ imaging in NTS astrocytes expressing a genetically encoded Ca^{2+} indicator. As 5-HT is also known to be released in the NTS from vagal afferent terminals to modulate glutamatergic transmission (Jeggo et al., 2005; Oskutyte et al., 2009; Hosford et al., 2015), the presence of 5-HT receptors on NTS glia was studied using $[Ca^{2+}]$ imaging *in vivo* and the identity of the NTS astroglial 5-HT receptor was determined *in vitro*. Finally, we investigated the importance of astroglial signalling mechanisms for the operation of cardiovascular reflexes by blocking Ca^{2+}-dependent vesicular release in NTS astrocytes in conscious rats with cardiovascular phenotyping and the assessment of baroreflex sensitivity.

Materials and Methods

The experiments were performed in Sprague Dawley rats in accordance with the European Commission Directive 2010/63/EU (European Convention for the Protection of Vertebrate Animals used for Experimental and Other Scientific Purposes) and the United Kingdom Home Office (Scientific Procedures) Act (1986) with project approval from the Institutional Animal Care and Use Committee of the University College London.

In vivo gene transfer

Young male Sprague Dawley rats (100-120 g) were anesthetized with a mixture of ketamine (60 mg of kg^{-1}, i.m.) and medetomidine (250 µg kg^{-1}, i.m.) and placed in a stereotaxic frame. NTS astrocytes were targeted bilaterally to express either a genetically encoded Ca^{2+} indicator GCaMP6 (to record activity) or dominant negative SNARE protein (dnSNARE) (to block vesicular exocytosis; Sheikhbahaei et al., 2018b).

Stable GCaMP6 expression along the rostro-caudal extent of the NTS was achieved by placing two microinjections per side (0.25 µl each, speed of injection 0.1 µl min^{-1}; coordinates from *calamus scriptorius* (i) 0.25 mm rostral, 0.5 mm lateral, 0.5 mm ventral and (ii) 0.75 mm rostral, 0.5 mm lateral, 0.5 mm ventral) of an adeno-associated viral vector (AAV) to express GCaMP6 under the control of an enhanced glial fibrillary acidic protein (GFAP) promoter

147 (AAV5.GfaABC1D.cytoGCaMP6f.SV40, titre $7x10^{11}$ viral particles mL^{-1}; University
148 of Pennsylvania Vector Core).
149
150 To block vesicular release mechanisms in NTS astrocytes, two microinjections
151 (0.25 µl each) per side of the adenoviral vector (AVV) with the enhanced GFAP
152 promoter (Liu et al., 2008) was used to drive the expression of dnSNARE (AVV-
153 sGFAP-dnSNARE-eGFP, titre $7.7x10^{9}$ viral particles mL^{-1}). Validation of
154 dnSNARE specificity and efficacy in blocking vesicular release mechanisms in
155 astrocytes was reported previously (Sheikhbahaei et al., 2018b).
156
157 To determine whether the effect of compromised astroglial function on
158 baroreflex sensitivity is specific to the NTS, in a separate group of animals
159 astrocytes of the ventrolateral medulla oblongata (VLM) were transduced to
160 express dnSNARE. This brainstem region contains pre-sympathetic and cardiac
161 vagal preganglionic neurons critical for the operation of the baroreflex.
162 Astrocytes within the VLM were targeted bilaterally with two microinjections per
163 side (1 µl each, 0.1 µl min^{-1}) of AVV-sGFAP-dnSNARE-eGFP using the following
164 coordinates from Bregma: 11 and 12 mm caudal, 2 mm lateral and 8.5 mm
165 ventral. In control animals, the astrocytes were targeted to express calcium
166 translocating channelrhodopsin variant (CatCh) fused with eGFP (vector: AVV-
167 sGFAP-CatCh-eGFP, titre $2.1x10^{9}$ viral particles mL^{-1}). Anesthesia was reversed
168 with atipamezole (1 mg kg^{-1}). No complications were observed after the surgery
169 and the animals gained weight normally.
170
171 *Anesthetized animal preparation and calcium imaging in NTS astrocytes in vivo*
172
173 Imaging experiments were conducted four weeks after the injections to allow a
174 high and stable level of GCaMP6 expression. Under isoflurane anesthesia (3% in
175 room air), the femoral artery and femoral vein were cannulated for the arterial
176 blood pressure recordings and the delivery of drugs, respectively. After gaining
177 vascular access, anesthesia was transitioned to α-chloralose (initial dose: 100
178 mg kg^{-1}, i.v., maintenance: 30 mg kg^{-1} h^{-1}, i.v.) and isoflurane was withdrawn. A
179 tracheotomy was performed and the animals were artificially ventilated using a
180 positive pressure rodent ventilator (tidal volume 8–10 ml kg^{-1}; frequency ~60
181 strokes min^{-1}). The body temperature was maintained at 37.0±0.5 °C with a

servo-controlled heating blanket. The head of the animal was secured in a stereotaxic frame. Arterial blood samples were taken regularly to monitor blood PO_2, PCO_2 and pH (RAPIDLab 348EX, Siemens). Inspired gas composition and/or rate/volume of the ventilation were adjusted to maintain arterial PO_2 within the range: 100-110 mmHg, PCO_2: 35-45 mmHg and pH: 7.35-7.45.

To record $[Ca^{2+}]_i$ responses in NTS astrocytes, the dorsal surface of the brainstem was exposed as described in detail previously (Gourine et al., 2008). $[Ca^{2+}]_i$ responses in the astrocytes evoked by electrical stimulation of the central end of the vagus nerve (5 s stimulation; 5 Hz, 0.8 mA, 10 ms pulse width) were recorded using a Leica fluorescence microscope and MiCAM02 high-resolution camera (SciMedia). To minimize movement artifacts, recordings were made under neuromuscular blockade with gallamine triethiodide (50 mg kg^{-1}, i.v.; then 10 mg kg^{-1} h^{-1}, i.v.). Under neuromuscular blockade, an adequate level anesthesia was ensured by constant monitoring of heart rate and blood pressure for signs of instability. Since acute changes in blood pressure in response to vagal stimulation were associated with drifts in focal plane affecting image acquisition, the arterial blood pressure was clamped by infusion of a nitric oxide synthase inhibitor Nω-Nitro-L-arginine methyl ester (L-NAME; 10 mg kg^{-1}, i.v.) and ganglion blocker chlorisondamine (1 mg kg^{-1} h^{-1}, i.v.). Four stimulations were applied: 2 control stimulations followed by stimulations in the presence of increasing doses of 5-HT_{2A} antagonist ketanserin given systemically (100 μg kg^{-1} and 300 μg kg^{-1}, i.v.). Stabilisation periods of 10 min between stimulations were allowed. In a separate set of experiments, stimulations were performed in the absence and presence of an AMPA receptor antagonist CNQX (10 mM in aCSF; applied topically to the dorsal brainstem). Imaging data were collected and analysed using MiCaM BV_Ana software.

Cell culture and calcium imaging in vitro

Primary astrocyte-enriched neuroglial cultures were prepared from the cortical, hippocampal, cerebellar, and dorsal brainstem tissue of rat pups (P2–P3 of either sex) as described previously (Kasymov et al., 2013). After isolation, the cells were plated on poly-D-lysine-coated coverslips and maintained at 37°C in a humidified atmosphere of 5% CO_2 and 95% air for a minimum of 12 d before the

experiments. Optical measurements of changes in $[Ca^{2+}]_i$ were performed using an inverted epifluorescence Olympus microscope equipped with a cooled CCD camera (Retiga; QImaging) as described previously (Angelova et al., 2015; Turovsky et al., 2016). We have found that from day 12 the cell cultures contained a negligible number of neurons. This was confirmed at the end of recordings by application of high potassium solution as described previously (Turovsky et al., 2015). Astrocytes show no $[Ca^{2+}]_i$ responses to K^+-induced depolarization or activity of the small number of neurons that may remain in the culture.

Experiments were performed in a custom-made flow-through imaging chamber in a standard HBSS containing 10 mM HEPES. To visualize $[Ca^{2+}]_i$ responses, astrocytes were loaded with a conventional Ca^{2+} indicator Fura-2 (5 μM; 30 min incubation; Invitrogen). After incubation with the dye, the culture medium was exchanged for fresh HBSS five times before commencing the imaging experiment. The effects of 5-HT or 5-HT receptor agonists on $[Ca^{2+}]_i$ in individual astrocytes were recorded. Excitation light was provided by a xenon arc lamp with the beam passing through a monochromator at 340 and 380 nm (Cairn Research) and emitted fluorescence at 515 nm was registered. Imaging data were collected and analysed using Andor software (Andor). All reported data were obtained from at least six separate experiments.

Recordings of the arterial blood pressure and heart rate using biotelemetry

Systemic arterial blood pressure and heart rate in conscious rats transduced to express dnSNARE or control transgene by the NTS and VLM astrocytes were recorded using biotelemetry, as described previously (Machhada et al., 2017). Rats were anesthetized with isoflurane (3% in O_2), a laparotomy was performed, and a catheter connected to a biotelemetry pressure transducer (model TA11PA-C40, DSI) was advanced rostrally into the abdominal aorta and secured in place with Vetbond (3M). The transmitter was secured to the abdominal wall and the incision was closed by successive suturing of the abdominal muscle and skin layers. For postoperative analgesia, the animals received carprofen (4 mg kg^{-1} d^{-1}; i.p.) for 2 days and were allowed to recover for at least 7 days. After the recovery period and following recordings of the

baseline hemodynamic parameters for 24 h, the animals received microinjections of the AVVs to express dnSNARE or control transgene in the NTS or VLM astrocytes, as described above. Blood pressure traces were recorded between 7 and 10 days after the injections of the viral vectors when the brainstem expression of the transgenes is fully established (Rajani et al., 2018; Sheikhbahaei et al., 2018b). Animals expressing dnSNARE in the VLM astrocytes were monitored for 24-hour period 7 days after the injections of viral vectors as the effect of targeting NTS astrocytes peaked at this time point.

Analysis of the biotelemetry data

Recordings of the arterial blood pressure were used to calculate the heart rate and spontaneous baroreflex gain (sBRG) for the light and dark periods of the 24h cycle. sBRG was determined from spontaneous changes in systolic blood pressure (SBP) and pulse interval (PI) as described in detail previously (Oosting et al., 1997; Waki et al., 2003).

Assessment of baroreceptor reflex gain (BRG) in anesthetized animals

In animals anesthetized with α-chloralose (initial dose of 100 mg kg^{-1}, i.v., maintained by 30 mg $kg^{-1}h^{-1}$, i.v.) and instrumented for the recordings of the arterial blood pressure and heart rate (as described above), arterial baroreceptors were activated by i.v. bolus injections of norepinephrine (1 μg kg^{-1}). Concomitant changes in blood pressure and heart rate were recorded from 3 consecutive stimulations delivered with intervals of 3 min. BRG was assessed in the absence and presence of $P2Y_1$ receptor antagonist MRS 2500 (5 μM) or agonist MRS 2365 (100 μM), applied on the dorsal surface of the brainstem. The BRG was calculated as a ratio of changes in HR to that of mean arterial blood pressure (bpm $mmHg^{-1}$) for reflex bradycardia. BRG values were averaged over 3 measurements made in control conditions and in the presence of either a $P2Y_1$ antagonist or agonist.

Histology and immunohistochemistry

At the end of the experiments, the animals were terminally anesthetised with

pentobarbitone sodium (200 mg kg^{-1}, i.p.) and perfused transracially with 0.1 M phosphate buffered saline (pH 7.4). The brainstem was removed and fixed for 24 h in 4% paraformaldehyde at 4 °C, followed by cryoprotection in 30% sucrose. Serial transverse sections (30 µm) of the medulla oblongata were cut using a freezing microtome. Immunohistochemistry was performed on free-floating sections by incubation overnight at 4 °C with mouse anti-MAP2 (1:500; Sigma, M1406), rabbit anti-TH (1:100; Sigma, HPA061003) and/or chicken anti-GFP (1:250; Aves Labs, Cat. GFP-1020) followed by incubation with secondary antibodies conjugated to the fluorescent probes for 2.5 h at room temperature (each 1:250; Life Science Technologies). Images were obtained with a confocal microscope (Zeiss LSM 900) or epiflorescent microscope (Leica DMR).

Drugs

5-HT receptor agonists and antagonists were used to identify the type of 5-HT receptors expressed by brainstem astrocytes: 5-HT_{2A} antagonists ketanserin and MDL 100907, 5-HT_{2A} agonist N,N-Dimethyltryptamine (DMT), 5-HT_{2B} agonist BW 723C86, 5-HT_{2C} agonist WAY 161503, 5-HT_3 antagonist granisetron. Phospholipase C activity was blocked with U73122. MRS 2365 and MRS 2500 were used to activate or inhibit $P2Y_1$ receptors, respectively. AMPA receptors were blocked with CNQX. All drugs were purchased from Tocris Bioscience.

Data analysis

Physiological data obtained in the experiments in anesthetized preparations were recorded and analyzed using *Spike2* software (Cambridge Electronic Design). Built-in analysis software tools (Olympus or MiCAM BV_Ana) were used to analyze the results of the imaging experiments. Differences between the experimental groups/treatments were tested for statistical significance by one-way or two-way ANOVA followed by the *post hoc* Tukey–Kramer test, Student's *t* test or Wilcoxon matched-pairs signed rank test, as appropriate. Data are reported as individual values and means ± SEM. Differences with $p<0.05$ were considered to be significant.

Results

Vagus nerve simulation activates NTS astrocytes in vivo

Strong expression of GCaMP6 was observed in astrocytes residing in the mediolateral and rostro-caudal extent of the dorsal vagal complex including the NTS, area postrema and dorsal motor nucleus of the vagus nerve (Fig. 1A). No colocalization between GCaMP6 expression (visualised by GFP immunoreactivity) and that of a neuronal marker microtubule-associated protein 2 (MAP2) (Matus, 1990) was observed, confirming specificity of astroglial targeting (Fig. 1B).

Rapid increases in GCaMP6 fluorescence intensity (0.98± 0.24 $\Delta F/F_0$; n=5) were recorded in response to short (5 s) electrical stimulation of the central end of the vagus nerve (Fig. 1D, E). The responses were observed in the area adjacent to the 4th ventricle, rostral from the *calamus scriptorius* (Fig. 1D, Movie 1) indicating that NTS astrocytes in the NTS respond to vagal afferent input with increases in intracellular [Ca^{2+}].

Brainstem astrocytes express 5-HT$_{2A}$ receptors

As there is evidence that 5-HT is co-released in the NTS with glutamate from vagal afferents (Ramage and Villalón, 2008), we tested for the presence of 5-HT receptors in cultured brainstem astrocytes. Astrocytes responded to application of 5-HT (10 μM) with profound elevations in intracellular [Ca^{2+}] (0.164±0.022 fura-2 ratio above the baseline, n=10; Fig. 2A). 5-HT-induced Ca^{2+} responses were not affected in the absence of extracellular Ca^{2+} (Ca^{2+}-free medium with the addition of 0.5 mM EGTA) (0.115±0.022, n=10, *t*-test, p=0.09; Fig. 2A), suggesting that 5-HT recruits Ca^{2+} from the intracellular stores, likely via activation of the G_q-coupled 5-HT$_2$ receptor subtype (Hoyer et al., 2002). Indeed, $[Ca^{2+}]_i$ responses triggered by 5-HT in the brainstem astrocytes were abolished in the presence of phospholipase-C (PLC) inhibitor U73122 (5 μM; 0.011±0.002 vs 0.340±0.054, n=15, *t*-test, p<0.001; Fig. 2B) and 5-HT$_{2A}$ receptor antagonist ketanserin (0.01 μM; 0.015±0.004 vs 0.172±0.014, n=16, *t*-test, p<0.001) (Fig. 2E). Neither 5-HT$_{2B}$ agonist BW723C86 (in concentrations 0.001-1 μM) nor 5-HT$_{2C}$ agonist WAY161503 (in concentrations 0.01-5 μM) had an effect on $[Ca^{2+}]_i$ in brainstem astrocytes (Fig. 2C, Fig. 2D). These data

indicated that responses of brainstem astrocytes to 5-HT are mediated by 5-HT_{2A} receptors (summarised in Fig. 2F).

For comparison, we analysed $[Ca^{2+}]_i$ responses induced by 5-HT in astrocytes residing in other areas of the brain (cerebellum, hippocampus and cortex; Fig 3). The results obtained suggest that the profile of 5-HT receptors expressed by brainstem astrocytes is distinct from that of the forebrain astrocytes. Similar to the brainstem astrocytes, $[Ca^{2+}]_i$ responses induced by 5-HT in cerebellar astrocytes (Bergmann glia) were blocked by U73122 or ketanserin (Fig. 3A and 3B). The 5-HT_{2C} agonist WAY161503 had no effect on Bergmann glia (Fig. 3C), suggesting that cerebellar astrocytes also express 5-HT_{2A} receptors. In contrast, $[Ca^{2+}]_i$ responses induced by 5-HT in hippocampal and cortical astrocytes were not affected by U73122 (Fig. 3D and 3G) or ketanserin (Fig. 3E), but were abolished in the presence of the 5-HT_3 antagonist granisetron (Fig. 3F and 3I). The 5-$HT_{2A/2C}$ receptor agonist DMT had no effect on $[Ca^{2+}]_i$ in cortical astrocytes (Fig. 3H). These data suggest that forebrain astrocytes express 5-HT_3 receptors and respond to 5-HT with $[Ca^{2+}]_i$ elevation mediated by Ca^{2+} entry from the extracellular space.

5-HT_{2A} receptors mediate $[Ca^{2+}]_i$ responses of NTS astrocytes evoked by vagus nerve simulation

To determine if 5-HT_{2A} receptors expressed by brainstem astrocytes are functional *in vivo*, we next studied the effect of 5-HT_{2A} receptor blockade on $[Ca^{2+}]_i$ responses of NTS astrocytes evoked by vagus nerve stimulation. Ketanserin dose-dependently decreased the amplitudes of $[Ca^{2+}]_i$ responses in NTS astrocytes evoked by stimulation of vagal afferents ($\Delta F/F_0$=0.65±0.2 and 0.46±0.16 from a baseline of 1.0±0.3 $\Delta F/F_0$; n=5, following administration i.v. in doses of 100 µg kg^{-1} and 300 µg kg^{-1}, respectively; n=5, one-way ANOVA, $p<0.01$; Fig. 4A-C, Movie 1, 2). In similar experimental conditions, $[Ca^{2+}]_i$ responses in NTS astrocytes evoked by vagus nerve simulation were abolished by AMPA receptor blockade with CNQX (10 mM; applied topically to the dorsal brainstem; Fig. 4D).

Blockade of vesicular release mechanisms in NTS astrocytes alters baroreflex sensitivity

To determine the functional significance of the recorded astroglial Ca^{2+} responses, we next determined whether blockade of Ca^{2+}-dependent vesicular release mechanisms in astrocytes of the NTS has an effect on baroreflex. In conscious freely moving rats, dnSNARE expression in astrocytes of the NTS (Fig. 5A) led to a significant increase in baroreflex sensitivity, when assessed 7 and 10 days after the injections of the viral vectors when the expression of the transgene peaked (Fig. 5B, sBRG 1.7±0.11 and 1.5±0.10 bpm $mmHg^{-1}$ vs 1.0±0.10 bpm $mmHg^{-1}$ at baseline, $p<0.001$). Baroreflex sensitivity was unaffected in animals transduced to express the control transgene in the NTS astrocytes (Fig. 5B, sBRG 1.1±0.08 and 1.1±0.13 bpm $mmHg^{-1}$ vs 1.0±0.07 bpm $mmHg^{-1}$ at baseline, $p<0.05$). Expression of dnSNARE or control transgene in astrocytes of the VLM (Fig. 5C) had no effect on baroreflex sensitivity (Fig. 5D).

$P2Y_1$ receptors in the NTS modulate the baroreflex

ATP is one of the main signalling molecules releases by astrocytes in response to elevations in $[Ca^{2+}]_i$ (Gourine and Kasparov, 2011). We next hypothesised that ATP is released by astrocytes in response to incoming afferent activity and acts on $P2Y_1$ receptors expressed by NTS inhibitory interneurons to restrain the expression of baroreflex. An analogous mechanism involving ATP-induced P2Y receptor-mediated activation of inhibitory interneurons has been described in the cortex (Wang et al., 2012). Baroreflex sensitivity was assessed in animals anesthetized with α-chloralose before and after application of a potent and selective $P2Y_1$ receptor agonist MRS 2365 (100 μM) or P2Y1 antagonist MRS 2500 (5 μM) (Kim et al., 2003) topically to the brainstem. Baroreflex was activated by bolus injections of norepinephrine. Activation of $P2Y_1$ receptors with MRS 2365 was found to reduce the baroreflex gain (Fig. 6A; 0.3±0.05 vs 0.5±0.05 bpm $mmHg^{-1}$ at baseline, $p=0.031$) while blockade of $P2Y_1$ receptors with MRS 2500 increased the baroreflex gain (Fig. 6B; 1.1±0.26 vs 0.7±0.15 bpm $mmHg^{-1}$ at baseline, $p=0.018$).

Discussion

The importance of astrocytes in supporting the function of NTS circuitry has been suggested previously by (Lin et al., 2013), who reported that ablation of NTS astrocytes using toxin saporin leads to cardiovascular reflex attenuation, lability of arterial pressure, damage of cardiac myocytes and, in some animals, sudden cardiac death. Considering the important role played by astrocytes in providing structural and metabolic support, as well as K^+ buffering and glutamate recycling, it is not surprising that physical ablation of astrocytes has a major impact on the neuronal function and, perhaps, nerve cell viability. Therefore, the role of astrocytes in the subtleties of neuronal information processing and afferent integration within the NTS remain unknown. In this study we aimed to determine the role of astrocytes in the NTS mechanisms that mediate the baroreceptor reflex pathway.

In vivo calcium imaging demonstrated that NTS astrocytes respond to vagal afferent input with increases in intracellular [Ca^{2+}]. These data are in agreement with the observations by McDougal and co-workers (2011) who reported that NTS astrocytes respond with increases in $[Ca^{2+}]_i$ to stimulation of the solitary tract in slices (McDougal et al., 2011). $[Ca^{2+}]_i$ responses in NTS astrocytes induced by vagus nerve stimulation were reduced or abolished by either 5-HT_{2A} or AMPA receptor blockade. This is consistent with the existing evidence that 5-HT is a co-transmitter released from vagal afferent terminals (Thor and Helke, 1989).

Previously, 5-HT receptors have been shown to be expressed by astrocytes in many brain areas (Sanden et al., 2000) but have not been identified in the brainstem astroglia. Pharmacological analysis of 5-HT-induced $[Ca^{2+}]_i$ responses in cultured brainstem astrocytes indicated that brainstem astrocytes express 5-HT_{2A} receptors (Fig. 2). Although 5-HT_3 receptors have been previously suggested to be expressed by NTS astrocytes (Huang et al., 2004), we found no evidence for their involvement in mediating the actions of 5-HT in brainstem astroglia. NTS astrocytes appear to be distinct from the forebrain astrocytes (cortical and hippocampal) where 5-HT effects are mediated solely by ionotropic

459 5-HT_3 receptors (Fig. 3).
460
461 The data obtained in this study show that 5-HT_{2A} receptors partially mediate
462 $[Ca^{2+}]_i$ responses in NTS astrocytes as these were reduced by ~50% in the
463 presence of 5-HT_{2A} antagonist ketanserin (Fig. 4). However, 5-HT released as a
464 result of vagal afferent activity alone was unable to trigger significant increases
465 in astrocytic $[Ca^{2+}]_i$, as blockade of AMPA receptors completely abolished these
466 responses. It is important to note that vagal afferents are not the only source of
467 5-HT in the NTS (Hosford et al., 2015). Tyrosine hydroxylase-expressing
468 (serotoninergic) neurons of the brainstem raphe send projections to the NTS and
469 could also be activated by reciprocal projections from the NTS (Thor and Helke,
470 1989; Rosin et al., 2006).
471
472 In an experiment involving specific blockade of Ca^{2+}-dependent vesicular release
473 machinery in the NTS astrocytes (by dnSNARE expression), we next determined
474 the functional significance of astroglial signalling in operation of the key
475 homeostatic reflex – the baroreceptor reflex (Fig. 5). It was found that inhibition
476 of Ca^{2+}-dependent astroglial signalling mechanisms increased the baroreflex
477 sensitivity when assessed in awake behaving rats. In order to determine
478 whether this effect is attributed specifically to the NTS astrocytes, we also
479 targeted the region of the ventrolateral medulla that harbours both pre-
480 sympathetic circuits (Marina et al., 2011) as well as cardiac vagal preganglionic
481 neurons of the nucleus ambiguus (Gourine et al., 2016), - both critically
482 important for the operation of the baroreflex. Interestingly, despite widespread
483 dnSNARE expression in astrocytes of the VLM, no effect on spontaneous
484 baroreflex gain was detected, indicating a very specific role for NTS astrocytes in
485 operation of this key cardiovascular reflex.
486
487 Our conclusions drawn from the data obtained in the experiments involving viral
488 gene transfer in brainstem astrocytes rely on GFAP promoter specificity. This
489 vector system has been validated and demonstrated to be highly specific in
490 targeting astroglial cells (Gourine et al., 2010; Rajani et al., 2018; Sheikhbahaei
491 et al., 2018b), albeit in other areas of the brainstem. Additional verification of
492 the expression specificity in the NTS showed that transgene expression is indeed
493 confined to non-neuronal cells; no cells expressing eGFP (reporter gene used in

494 both viral vectors) showed MAP2 immunoreactivity (Fig. 1B, Fig. 5A, Fig. 5C).
495 Further, expression of the virial vectors and the actions of the pharmacological
496 agents used in characterisation of the baroreflex in this study are not confined to
497 the NTS, rather the dorsal vagal complex. There is strong $P2Y_1$ receptor presence
498 throughout the dorsal vagal complex, including the area postrema (Fong et al.,
499 2002), the area shown to modulate the baroreflex via projections to the NTS
500 (Shapiro and Miselis, 1985; Johnson and Gross, 1993). However, the area
501 postrema does not seem to be directly involved in the baroreflex pathway but
502 can modulate NTS circuit activity by responding to various circulating factors, as
503 it is positioned outside the blood-brain barrier (Tan et al., 2007). Additionally,
504 the dorsal vagal motor nucleus (DVMN) may modulate the baroreflex, but only in
505 the pathophysiological context, such as in conditions of systemic arterial
506 hypertension (Moreira et al., 2018). Taken together, the data obtained in the
507 present study strongly suggest that the NTS is the dorsal brainstem site where
508 the altered astroglial function modulates the expression of baroreflex.
509
510 One of the main astroglial signalling molecules is recognised to be ATP, which is
511 known to inhibit local neuronal activity indirectly following rapid breakdown to
512 adenosine, - the mechanism first reported to operate in retina (Newman, 2003).
513 Indeed, activation of adenosine A_1 receptors in the NTS inhibits baroreflex
514 (Scislo and O'Leary, 2005). However, the data obtained in this study suggested
515 the existence of a different mechanism, which is independent of adenosine
516 actions. Pharmacological inhibition of $P2Y_1$ receptors was found to have a similar
517 effect on baroreflex as blockade of Ca^{2+}-dependent vesicular release in NTS
518 astrocytes expressing dnSNARE. These data suggest that, upon activation by
519 afferent input, the NTS astrocytes release ATP which acts on NTS inhibitory
520 neurons expressing $P2Y_1$ receptors, - a mechanism analogous to that described
521 by (Wang et al., 2012) in the cortex. It is also worth noting that ADP is the more
522 potent ligand of the $P2Y_1$ receptor (Waldo and Harden, 2004), therefore, the
523 signalling pathway proposed could require (or be potentiated by) breakdown of
524 ATP to ADP by ectonucleotidases encountered in the extracellular space.
525
526 Baroreceptor reflex is critically important for the short term (beat-to-beat)
527 control of the arterial blood pressure. There is strong evidence that impaired
528 baroreflex function contributes to the development of cardiovascular disease and

serves as a robust predictor of cardiovascular and all-cause mortality (La Rovere et al., 1998; La Rovere et al., 2001; McCrory et al., 2016). The mechanisms underlying impairment of baroreflex function in pathological conditions remain largely unknown. Previously proposed central mechanisms may involve activation of the cardiac sympathetic afferent reflex which alters the baroreflex via angiotensin II type 1 receptors in the NTS (Kasparov and Paton, 1999; Gao et al., 2005), and/or reduction of brain-derived neurotropic factor (BDNF) neurotransmission in the NTS (Becker et al., 2016). The results of the present study offer another plausible mechanism. Various pathological conditions that are associated with the development of the systemic and central inflammatory response leading to activation of NTS glia (astro- and microglia) would be expected to facilitate the release of ATP, increase the concentration of ATP/ADP in the extracellular milieu and inhibit the baroreflex centrally. Indeed, activation of astrocytes and reactive astrogliosis have been reported after the CNS trauma, infection, ischemia, stroke and in autoimmune disease (reviewed by Sofroniew and Vinters, 2010). Higher level of "ambient" ATP released by activated astrocytes and microglia would be expected to reduce the baroreflex sensitivity via $P2Y_1$ receptor-mediated NTS mechanism described here.

Additionally, repeated activation of chemosensory inputs had been shown to inhibit the baroreflex and is thought to contribute to the pathology of conditions such as sleep apnoea (see Mifflin et al., 2015). Activation of chemosensory inputs increases extracellular 5-HT concentration in the NTS via release from afferent terminals, and also by the inputs from the central chemosensory sites (Kellett et al., 2005; Wu et al., 2019). This would be expected to maintain "activation" of astrocytes and decrease the baroreflex sensitivity. Previous studies of the role of 5-HT_2 receptors within the NTS suggested that the astrocytic 5-HT_{2A} pathway is unlikely to be active under normal physiological conditions. Indeed, there is evidence that 5-HT_{2A} receptor blockade in the NTS did not alter the baroreflex sensitivity (Sevoz-Couche et al., 2006; Comet et al., 2007). However, these studies also reported a facilitatory effect of 5-HT_{2A} receptor activation on baroreflex. It is possible that the 5-HT_{2A} receptors expressed by astrocytes are recruited primarily in pathophysiological conditions discussed above and, only in these circumstances, modify the baroreflex *via* astrocytic release of ATP.

In conclusion, the data obtained in the present study suggest that astrocytes are integral components of the NTS mechanisms which process incoming afferent information. NTS astrocytes are activated by glutamate (McDougal et al., 2011) and 5-HT released by vagal afferent fibres and acting at AMPA and 5-HT_{2A} receptors, respectively (Fig. 7). Activation of astrocytes in response to afferent stimulation leads to the release of ATP acting on $P2Y_1$ receptors to modulate the baroreflex sensitivity. Together, the results of this study add to the growing body of evidence supporting an active role of astrocytes in the information processing in the central nervous system.

Acknowledgements

Supported by The Wellcome Trust. A.V.G. is a Wellcome Trust Senior Research Fellow (Ref: 095064) and British Heart Foundation (Refs: PG/13/79/30429, RG/14/4/30736 and RG/19/5/34463). S.M. is a Marie Skłodowska-Curie Research Fellow (Ref: 654691).

References

Angelova PR, Kasymov V, Christie I, Sheikhbahaei S, Turovsky E, Marina N, Korsak A, Zwicker J, Teschemacher AG, Ackland GL, Funk GD, Kasparov S, Abramov AY, Gourine AV (2015) Functional Oxygen Sensitivity of Astrocytes. The Journal of Neuroscience 35:10460.

Baude A, Strube C, Tell F, Kessler J-P (2009) Glutamatergic neurotransmission in the nucleus tractus solitarii: Structural and functional characteristics. Journal of Chemical Neuroanatomy 38:145-153.

Becker BK, Tian C, Zucker IH, Wang H-J (2016) Influence of brain-derived neurotrophic factor-tyrosine receptor kinase B signalling in the nucleus tractus solitarius on baroreflex sensitivity in rats with chronic heart failure. The Journal of Physiology 594:5711-5725.

Comet MA, Bernard JF, Hamon M, Laguzzi R, Sevoz-Couche C (2007) Activation of nucleus tractus solitarius 5-HT2A but not other 5-HT2 receptor

596 subtypes inhibits the sympathetic activity in rats. Eur J Neurosci 26:345-
597 354.
598 Dallaporta M, Bonnet MS, Horner K, Trouslard J, Jean A, Troadec JD (2010) Glial
599 cells of the nucleus tractus solitarius as partners of the dorsal hindbrain
600 regulation of energy balance: a proposal for a working hypothesis. Brain
601 Res 1350:35-42.
602 Fong AY, Krstew EV, Barden J, Lawrence AJ (2002) Immunoreactive localisation
603 of P2Y1 receptors within the rat and human nodose ganglia and rat
604 brainstem: comparison with [alpha 33P]deoxyadenosine 5'-triphosphate
605 autoradiography. Neuroscience 113:809-823.
606 Gao L, Schultz Harold D, Patel Kaushik P, Zucker Irving H, Wang W (2005)
607 Augmented Input From Cardiac Sympathetic Afferents Inhibits Baroreflex
608 in Rats With Heart Failure. Hypertension 45:1173-1181.
609 Gourine AV, Kasparov S (2011) Astrocytes as brain interoceptors. Experimental
610 Physiology 96:411-416.
611 Gourine AV, Machhada A, Trapp S, Spyer KM (2016) Cardiac vagal preganglionic
612 neurones: An update. Auton Neurosci 199:24-28.
613 Gourine AV, Dale N, Korsak A, Llaudet E, Tian F, Huckstepp R, Spyer KM (2008)
614 Release of ATP and glutamate in the nucleus tractus solitarii mediate
615 pulmonary stretch receptor (Breuer–Hering) reflex pathway. The Journal
616 of Physiology 586:3963-3978.
617 Gourine AV, Kasymov V, Marina N, Tang F, Figueiredo MF, Lane S,
618 Teschemacher AG, Spyer KM, Deisseroth K, Kasparov S (2010) Astrocytes
619 Control Breathing Through pH-Dependent Release of ATP. Science
620 329:571-575.
621 Halassa MM, Florian C, Fellin T, Munoz JR, Lee S-Y, Abel T, Haydon PG, Frank
622 MG (2009) Astrocytic Modulation of Sleep Homeostasis and Cognitive
623 Consequences of Sleep Loss. Neuron 61:213-219.
624 Han J, Kesner P, Metna-Laurent M, Duan T, Xu L, Georges F, Koehl M, Abrous
625 Djoher N, Mendizabal-Zubiaga J, Grandes P, Liu Q, Bai G, Wang W, Xiong
626 L, Ren W, Marsicano G, Zhang X (2012) Acute Cannabinoids Impair
627 Working Memory through Astroglial CB1 Receptor Modulation of
628 Hippocampal LTD. Cell 148:1039-1050.
629 Hosford PS, Ramage AG (2019) Involvement of 5-HT in Cardiovascular Afferent
630 Modulation of Brainstem Circuits Involved in Blood Pressure Maintenance.

631 In: Serotonin the mediator that spans evolution (Pilowsky PM, ed), pp
632 239-270: Academic Press Elsevier.
633 Hosford PS, Millar J, Ramage AG (2015) Cardiovascular afferents cause the
634 release of 5-HT in the nucleus tractus solitarii; this release is regulated by
635 the low- (PMAT) not the high-affinity transporter (SERT). The Journal of
636 Physiology 593:1715-1729.
637 Hoyer D, Hannon JP, Martin GR (2002) Molecular, pharmacological and
638 functional diversity of 5-HT receptors. Pharmacology Biochemistry and
639 Behavior 71:533-554.
640 Huang J, Spier AD, Pickel VM (2004) 5-HT3A receptor subunits in the rat medial
641 nucleus of the solitary tract: subcellular distribution and relation to the
642 serotonin transporter. Brain Research 1028:156-169.
643 Jeggo RD, Kellett DO, Wang Y, Ramage AG, Jordan D (2005) The role of central
644 5-HT3 receptors in vagal reflex inputs to neurones in the nucleus tractus
645 solitarius of anaesthetized rats. J Physiol 566:939-953.
646 Johnson AK, Gross PM (1993) Sensory circumventricular organs and brain
647 homeostatic pathways. FASEB J 7:678-686.
648 Kasparov S, Paton JF (1999) Differential effects of angiotensin II in the nucleus
649 tractus solitarii of the rat--plausible neuronal mechanism. J Physiol 521 Pt
650 1:227-238.
651 Kasymov V, Larina O, Castaldo C, Marina N, Patrushev M, Kasparov S, Gourine
652 AV (2013) Differential Sensitivity of Brainstem versus Cortical Astrocytes
653 to Changes in pH Reveals Functional Regional Specialization of Astroglia.
654 The Journal of Neuroscience 33:435.
655 Kellett DO, Ramage AG, Jordan D (2005) Central 5-HT7 receptors are critical for
656 reflex activation of cardiac vagal drive in anaesthetized rats. J Physiol
657 563:319-331.
658 Kim HS, Ohno M, Xu B, Kim HO, Choi Y, Ji XD, Maddileti S, Marquez VE, Harden
659 TK, Jacobson KA (2003) 2-Substitution of adenine nucleotide analogues
660 containing a bicyclo[3.1.0]hexane ring system locked in a northern
661 conformation: enhanced potency as P2Y1 receptor antagonists. J Med
662 Chem 46:4974-4987.
663 La Rovere MT, Bigger JT, Marcus FI, Mortara A, Schwartz PJ (1998) Baroreflex
664 sensitivity and heart-rate variability in prediction of total cardiac mortality
665 after myocardial infarction. The Lancet 351:478-484.

La Rovere MT, Pinna Gian D, Hohnloser Stefan H, Marcus Frank I, Mortara A, Nohara R, Bigger JT, Camm AJ, Schwartz Peter J (2001) Baroreflex Sensitivity and Heart Rate Variability in the Identification of Patients at Risk for Life-Threatening Arrhythmias. Circulation 103:2072-2077.

Lin L-H, Moore SA, Jones SY, McGlashon J, Talman WT (2013) Astrocytes in the Rat Nucleus Tractus Solitarii Are Critical for Cardiovascular Reflex Control. The Journal of Neuroscience 33:18608-18617.

Liu B, Paton JF, Kasparov S (2008) Viral vectors based on bidirectional cell-specific mammalian promoters and transcriptional amplification strategy for use in vitro and in vivo. BMC Biotechnol 8:49.

Machhada A, Trapp S, Marina N, Stephens RCM, Whittle J, Lythgoe MF, Kasparov S, Ackland GL, Gourine AV (2017) Vagal determinants of exercise capacity. Nat Commun 8:15097.

Marina N, Abdala AP, Korsak A, Simms AE, Allen AM, Paton JF, Gourine AV (2011) Control of sympathetic vasomotor tone by catecholaminergic C1 neurones of the rostral ventrolateral medulla oblongata. Cardiovasc Res 91:703-710.

Matus A (1990) Microtubule-associated proteins and the determination of neuronal form. J Physiol (Paris) 84:134-137.

McCrory C, Berkman Lisa F, Nolan H, O'Leary N, Foley M, Kenny Rose A (2016) Speed of Heart Rate Recovery in Response to Orthostatic Challenge. Circulation Research 119:666-675.

McDougal DH, Hermann GE, Rogers RC (2011) Vagal Afferent Stimulation Activates Astrocytes in the Nucleus of the Solitary Tract Via AMPA Receptors: Evidence of an Atypical Neural–Glial Interaction in the Brainstem. The Journal of Neuroscience 31:14037-14045.

Mifflin S, Cunningham JT, Toney GM (2015) Neurogenic mechanisms underlying the rapid onset of sympathetic responses to intermittent hypoxia. J Appl Physiol (1985) 119:1441-1448.

Moreira TS, Antunes VR, Falquetto B, Marina N (2018) Long-term stimulation of cardiac vagal preganglionic neurons reduces blood pressure in the spontaneously hypertensive rat. J Hypertens 36:2444-2452.

Navarrete M, Perea G, de Sevilla DF, Gómez-Gonzalo M, Núñez A, Martín ED, Araque A (2012) Astrocytes Mediate In Vivo Cholinergic-Induced Synaptic Plasticity. PLOS Biology 10:e1001259.

701 Newman EA (2003) Glial cell inhibition of neurons by release of ATP. J Neurosci
702 23:1659-1666.
703 Oosting J, Struijker-Boudier HAJ, Janssen BJA (1997) Validation of a continuous
704 baroreceptor reflex sensitivity index calculated from spontaneous
705 fluctuations of blood pressure and pulse interval in rats. Journal of
706 Hypertension 15:391-399.
707 Oskutyte D, Jordan D, Ramage AG (2009) Evidence that 5-hydroxytryptamine(7)
708 receptors play a role in the mediation of afferent transmission within the
709 nucleus tractus solitarius in anaesthetized rats. Br J Pharmacol 158:1387-
710 1394.
711 Rajani V, Zhang Y, Jalubula V, Rancic V, SheikhBahaei S, Zwicker JD, Pagliardini
712 S, Dickson CT, Ballanyi K, Kasparov S, Gourine AV, Funk GD (2018)
713 Release of ATP by pre-Botzinger complex astrocytes contributes to the
714 hypoxic ventilatory response via a Ca(2+) -dependent P2Y1 receptor
715 mechanism. J Physiol 596:3245-3269.
716 Ramage AG, Villalón CM (2008) 5-Hydroxytryptamine and cardiovascular
717 regulation. Trends in Pharmacological Sciences 29:472-481.
718 Rosin DL, Chang DA, Guyenet PG (2006) Afferent and efferent connections of
719 the rat retrotrapezoid nucleus. J Comp Neurol 499:64-89.
720 Sanden N, Thorlin T, Blomstrand F, Persson PA, Hansson E (2000) 5-
721 Hydroxytryptamine2B receptors stimulate Ca2+ increases in cultured
722 astrocytes from three different brain regions. Neurochem Int 36:427-434.
723 Scislo TJ, O'Leary DS (2005) Purinergic mechanisms of the nucleus of the
724 solitary tract and neural cardiovascular control. Neurol Res 27:182-194.
725 Sevoz-Couche C, Brouillard C (2017) Key role of 5-HT3 receptors in the nucleus
726 tractus solitarii in cardiovagal stress reactivity. Neurosci Biobehav Rev
727 74:423-432.
728 Sevoz-Couche C, Comet MA, Bernard JF, Hamon M, Laguzzi R (2006) Cardiac
729 baroreflex facilitation evoked by hypothalamus and prefrontal cortex
730 stimulation: role of the nucleus tractus solitarius 5-HT2A receptors. Am J
731 Physiol Regul Integr Comp Physiol 291:R1007-1015.
732 Shapiro RE, Miselis RR (1985) The central neural connections of the area
733 postrema of the rat. J Comp Neurol 234:344-364.

734 SheikhBahaei S, Morris B, Collina J, Anjum S, Znati S, Gamarra J, Zhang R,
735 Gourine AV, Smith JC (2018a) Morphometric analysis of astrocytes in
736 brainstem respiratory regions. J Comp Neurol 526:2032-2047.
737 Sheikhbahaei S, Turovsky EA, Hosford PS, Hadjihambi A, Theparambil SM, Liu B,
738 Marina N, Teschemacher AG, Kasparov S, Smith JC, Gourine AV (2018b)
739 Astrocytes modulate brainstem respiratory rhythm-generating circuits and
740 determine exercise capacity. Nature Communications 9:370.
741 Sofroniew MV, Vinters HV (2010) Astrocytes: biology and pathology. Acta
742 neuropathologica 119:7-35.
743 Talman WT (1997) Glutamatergic transmission in the nucleus tractus solitarii:
744 from server to peripherals in the cardiovascular information
745 superhighway. Brazilian Journal of Medical and Biological Research 30:1-
746 7.
747 Tan PS, Killinger S, Horiuchi J, Dampney RA (2007) Baroreceptor reflex
748 modulation by circulating angiotensin II is mediated by AT1 receptors in
749 the nucleus tractus solitarius. Am J Physiol Regul Integr Comp Physiol
750 293:R2267-2278.
751 Thor KB, Helke CJ (1989) Serotonin and substance P colocalization in medullary
752 projections to the nucleus tractus solitarius: dual-colour
753 immunohistochemistry combined with retrograde tracing. J Chem
754 Neuroanat 2:139-148.
755 Turovsky E, Karagiannis A, Abdala AP, Gourine AV (2015) Impaired CO2
756 sensitivity of astrocytes in a mouse model of Rett syndrome. J Physiol
757 593:3159-3168.
758 Turovsky E, Theparambil SM, Kasymov V, Deitmer JW, del Arroyo AG, Ackland
759 GL, Corneveaux JJ, Allen AN, Huentelman MJ, Kasparov S, Marina N,
760 Gourine AV (2016) Mechanisms of CO_2/H^+ Sensitivity of Astrocytes. The
761 Journal of Neuroscience 36:10750.
762 Waki H, Kasparov S, Wong L-F, Murphy D, Shimizu T, Paton JFR (2003) Chronic
763 inhibition of endothelial nitric oxide synthase activity in nucleus tractus
764 solitarii enhances baroreceptor reflex in conscious rats. The Journal of
765 Physiology 546:233-242.
766 Waldo GL, Harden TK (2004) Agonist binding and Gq-stimulating activities of the
767 purified human P2Y1 receptor. Mol Pharmacol 65:426-436.

768 Wang F, Smith NA, Xu Q, Fujita T, Baba A, Matsuda T, Takano T, Bekar L,
769 Nedergaard M (2012) Astrocytes Modulate Neural Network Activity by
770 Ca2+-Dependent Uptake of Extracellular K+. Science Signaling 5:ra26.
771 Wu Y, Proch KL, Teran FA, Lechtenberg RJ, Kothari H, Richerson GB (2019)
772 Chemosensitivity of Phox2b-expressing retrotrapezoid neurons is
773 mediated in part by input from 5-HT neurons. J Physiol.
774

Figure legends

Figure 1. *In vivo* imaging of Ca^{2+} responses in astrocytes of the nucleus of the solitary tract (NTS). (***A***) Schematic drawing of the rat brain in sagittal projection illustrating the anatomical location of the NTS targeted to express GCaMP6 in astrocytes under the control of GFAP promoter GfaABC1D (vector AAV5.GfaABC1D.cytoGCaMP6f.SV40); GCaMP6 expression by astrocytes in the dorsal vagal complex 4 weeks after transfection. AP, area postrema; 4V, 4^{th} ventricle. Distance from bregma (in mm) is indicated. (***B****)* Confocal images illustrating NTS astrocytes expressing GCaMP6 (identified by eGFP-immunoreactivity) with no co-localization of expression with MAP2-immunoreactivity (neuronal marker); (***C***) Schematic drawing of the recording setup that included a CCD camera coupled to a low-power microscope to obtain fluorescent images from the dorsal aspect of the brainstem. The central end of the vagus nerve was stimulated electrically. (***D***) False color images of GCaMP6 fluorescence at baseline and at the peak of the response evoked by vagus nerve stimulation. Colored boxes depict regions of interest. (***E***) Representative changes in GCaMP6 fluorescence in 4 areas of interest (indicated in D) evoked by electrical stimulation of the ipsilateral vagus nerve (VNS).

Figure 2. Brainstem astrocytes in culture respond to 5-HT with increases in $[Ca^{2+}]_i$ *via* activation of $5\text{-}HT_{2A}$ receptors. (***A***) Brainstem astrocytes respond to 5-HT (10 μM) with elevations in $[Ca^{2+}]_i$. 5-HT-induced $[Ca^{2+}]_i$ responses are independent of extracellular Ca^{2+}. (***B***) 5-HT-induced $[Ca^{2+}]_i$ responses are blocked in the presence of a PLC-inhibitor U73122 (5 μM). (***C***) Brainstem astrocytes do not respond to $5\text{-}HT_{2B}$ receptor agonist BW723C86 and (***D***) $5\text{-}HT_{2c}$ receptor agonist WAY161503. (***E***) 5-HT-induced $[Ca^{2+}]_i$ responses are blocked in the presence of $5\text{-}HT_{2A}$ receptor antagonist ketanserin (0.01 μM). (***F***) Summary data illustrating peak $[Ca^{2+}]_i$ responses in the brainstem astrocytes induced by 5-HT, 5-HT receptor agonists (BW723C86, 1 μM and WAY161503, 5 μM) and 5-HT in Ca^{2+}-free conditions and in the presence of ketanserin (Student's t-test).

Figure 3. Distinct receptors mediate 5-HT-induced $[Ca^{2+}]_i$ responses in astrocytes residing in different parts of the central nervous system. **Cerebellar astrocytes** express $5\text{-}HT_{2A}$ receptors: (***A***) 5-HT (10 μM)-induced $[Ca^{2+}]_i$ responses in cultured cerebellar astrocytes are blocked by U73122 (5 μM) and

(***B***) 5-HT_{2A} antagonist ketanserin (0.01 μM). (***C***) Cerebellar astrocytes do not respond to 5-HT_{2c} receptor agonist WAY161503 (0.1-5 μM). **Hippocampal astrocytes** express 5-HT_3 receptors: (***D***) 5-HT-evoked $[Ca^{2+}]_i$ responses in hippocampal astrocytes are unaffected by U73122 (10 μM) (***E***) 5-HT evoked $[Ca^{2+}]_i$ responses in hippocampal astrocytes are unaffected by ketanserin (0.01 μM) but are blocked by (***F***) 5-HT_3 antagonist granisetron (20 μM). **Cortical astrocytes** express 5-HT_3 receptors: (***G***) 5-HT- evoked $[Ca^{2+}]_i$ responses in cortical astrocytes are unaffected by U73122 (5 μM) and do not respond to (***H***) 5-HT_2 receptor agonist N,N-Dimethyltryptamine (DMT, 0.5-10 μM). (***I***) 5-HT-evoked $[Ca^{2+}]_i$ responses in cortical astrocytes are blocked by 5-HT_3 antagonist granisetron (20 μM).

Figure 4. Ca^{2+} responses in NTS astrocytes induced by vagus nerve stimulation (VNS) are mediated by 5-HT and glutamate. (***A****)* Representative recordings illustrating changes in GCaMP6 fluorescence (±SEM) reporting $[Ca^{2+}]_i$ dynamics in response to VNS in the absence (control conditions 1 and 2 separated by 10 min intervals) and presence of 5-HT_{2A} receptor antagonist ketanserin (Ket, 100 or 300 μg kg^{-1}, i.v.; n=5) (***B***) Representative false color images of peak increases in GCaMP6 fluorescence induced by VNS in the absence and presence of ketanserin. 4V, fourth ventricle. (***C***) Summary data illustrating the effect of ketanserin on peak $[Ca^{2+}]_i$ responses induced by VNS in the NTS astrocytes (one-way ANOVA followed by Sidak's multiple comparisons test). (***D***) Representative recordings and false color images illustrating changes in GCaMP6 fluorescence in response to VNS in the absence and presence of an AMPA receptor antagonist CNQX (10 mM, topical application).

Figure 5. Dominant negative SNARE protein (dnSNARE) expression in NTS astrocytes increases baroreflex sensitivity. (***A***) Photomicrographs of the coronal sections of the rat brainstem illustrating the expression of dnSNARE in astrocytes of the NTS and wider dorsal vagal complex. Astrocytes expressing the transgenes were identified by eGFP fluorescence. Schematic drawings illustrate the spatial extent of dnSNARE expression. Distance from bregma (in mm) is indicated. Higher-magnification image of dnSNARE-eGFP expression (green) in

astrocytes of the intermediate NTS shows no co-localization of expression with MAP2-immunoreactivity (red). AP, area postrema. Gr, gracile nucleus (***B***) Summary data illustrating values of spontaneous baroreceptor gain (sBRG) in conscious freely-moving animals transduced to express the control transgene (CatCh-eGFP) or dnSNARE in the NTS astrocytes (one-way ANOVA). (***C***) Photomicrographs of the coronal sections of the rat brainstem illustrating the expression of dnSNARE in astrocytes of the ventrolateral medulla oblongata (VLM). Pre-sympathetic neurons of the VLM are identified by tyrosine hydroxylase immunoreactivity (TH-IR). Schematic drawings illustrate the spatial extent of dnSNARE expression in the VLM region. Distance from bregma (in mm) is indicated. Higher-magnification image of dnSNARE-eGFP expression (green) in the VLM shows no co-localization of expression with MAP2-immunoreactivity (red). LS, left side. RS, right side. NA, nucleus ambiguus. (***D***) Summary data illustrating values of sBRG in conscious freely-moving animals transduced to express CatCh-eGFP or dnSNARE in astrocytes of the ventrolateral medulla oblongata (one-way ANOVA).

Figure 6. $P2Y_1$ receptors in the NTS modulate baroreflex sensitivity. (***A***) $P2Y_1$ receptor agonist MRS 2365 (100 μM, topical application on the dorsal brainstem surface) inhibits bradycardia induced by baroreceptor activation with systemic norepinephrine (NA; 0.1 μg kg^{-1}, i.v.) in anesthetized rats (Wilcoxon matched-pairs signed rank test). (***B***) $P2Y_1$ receptor antagonist MRS 2500 (5 μM, topical application on the dorsal brainstem surface) potentiates the bradycardia induced by baroreceptor activation with systemic NA (0.1 μg kg^{-1}, i.v.) in anesthetized rats (Wilcoxon matched-pairs signed rank test). BP, arterial blood pressure. HR, heart rate. BRG, baroreceptor gain. Representative responses recorded before and 15 minutes after each drug application are shown.

Figure 7. Schematic drawing of the proposed NTS mechanisms involved in modulation of the baroreflex. Vagal afferent terminals release 5-HT and glutamate acting on 2^{nd} order relay neurons and astrocytes in the NTS. In response to incoming afferent information, NTS astrocytes release ATP which restricts the expression of baroreflex via activation of $P2Y_1$ receptors on local inhibitory interneurons. ST, solitary tract. AP, area postrema. 4V, 4^{th} ventricle.

879 VLM, ventrolateral medulla. NA, nucleus ambiguus. X, vagus nerve. IX,
880 glossopharyngeal nerve.
881
882 ***Movie 1.*** Representative recording of astrocytic intracellular calcium activity in
883 the NTS during vagal nerve stimulation under control conditions.
884
885 ***Movie 2.*** Representative recording of astrocytic intracellular calcium activity in
886 the NTS during vagal nerve stimulation 10 min after application of 300 µg kg^{-1}
887 ketanserin (i.v.).

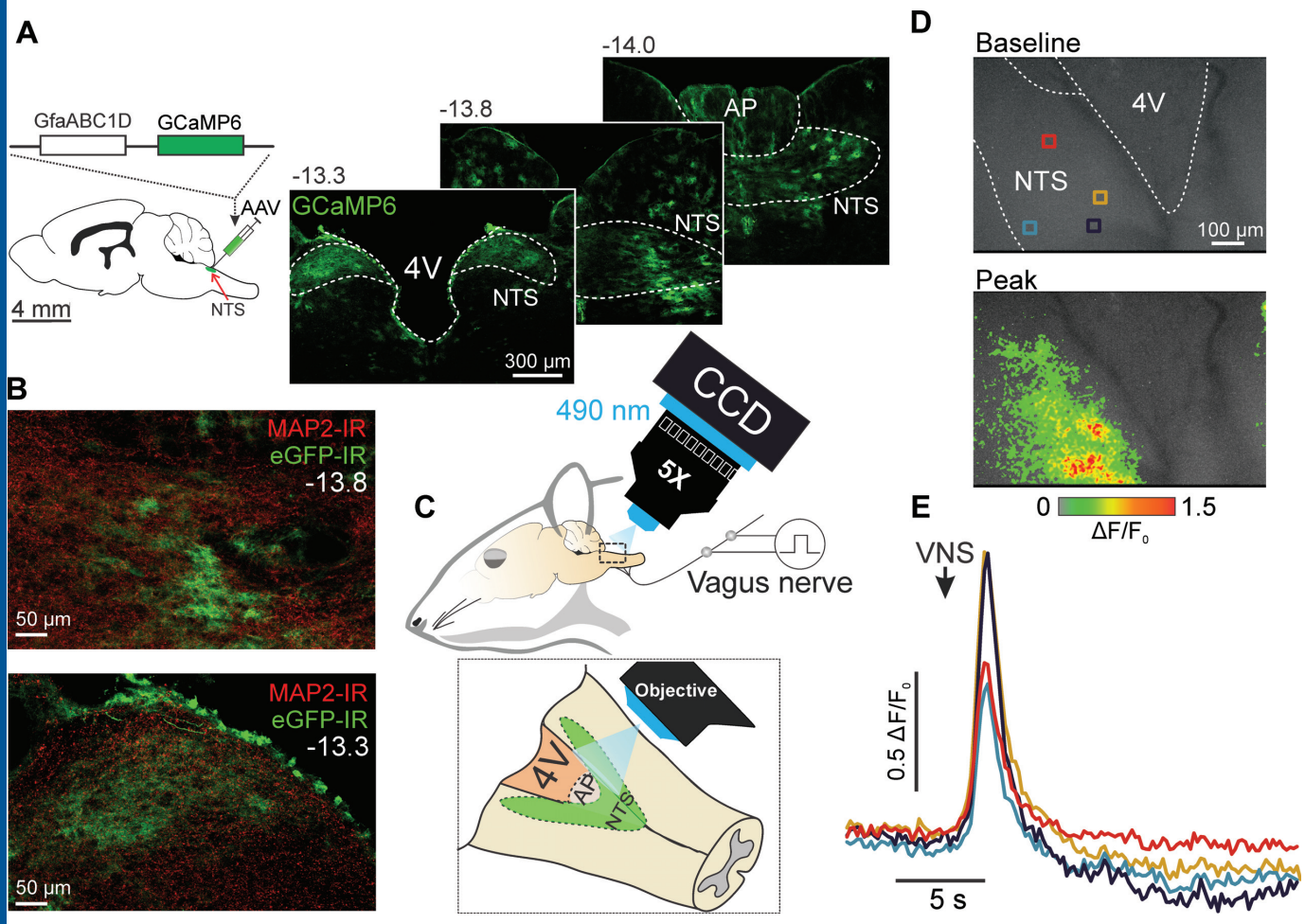

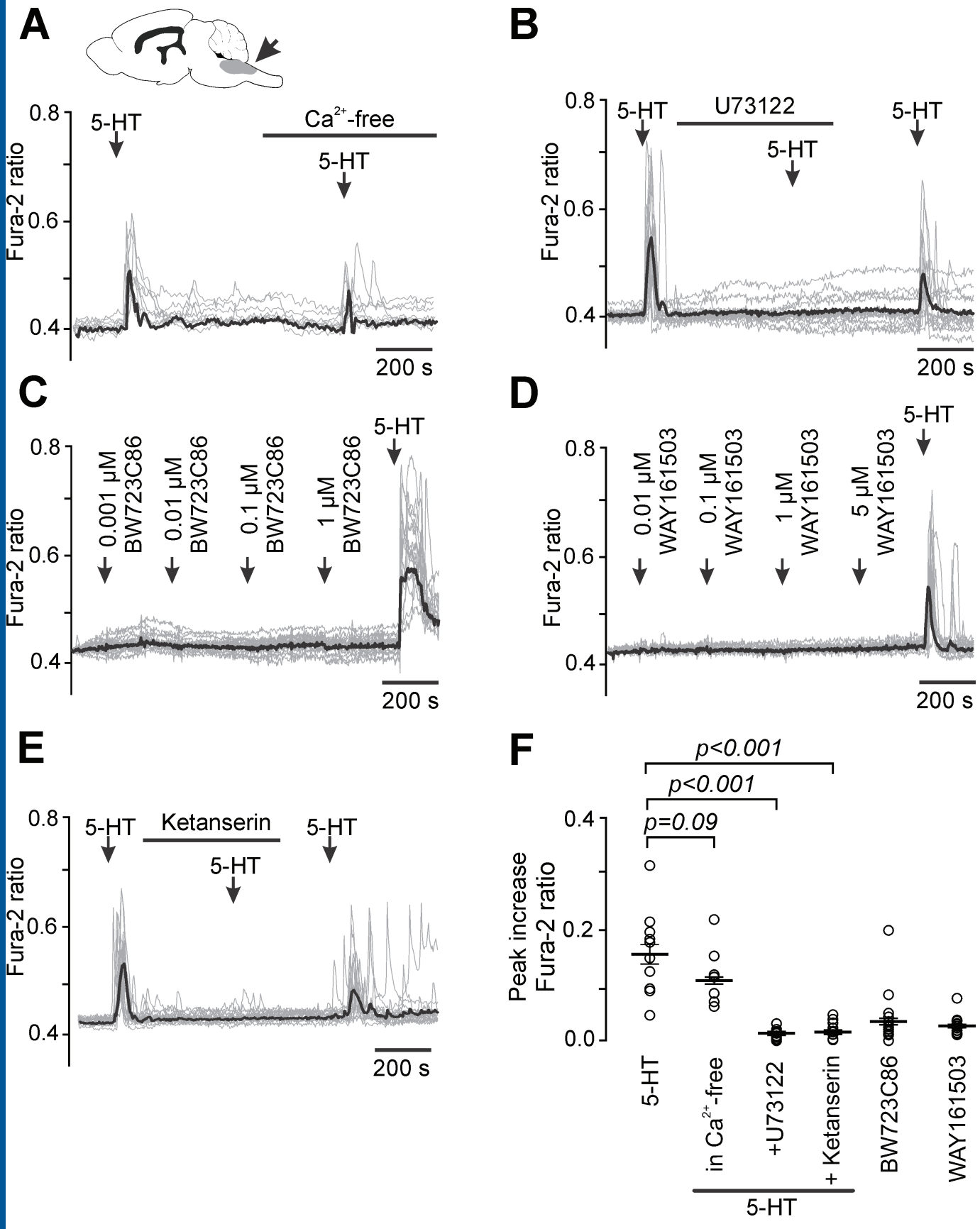

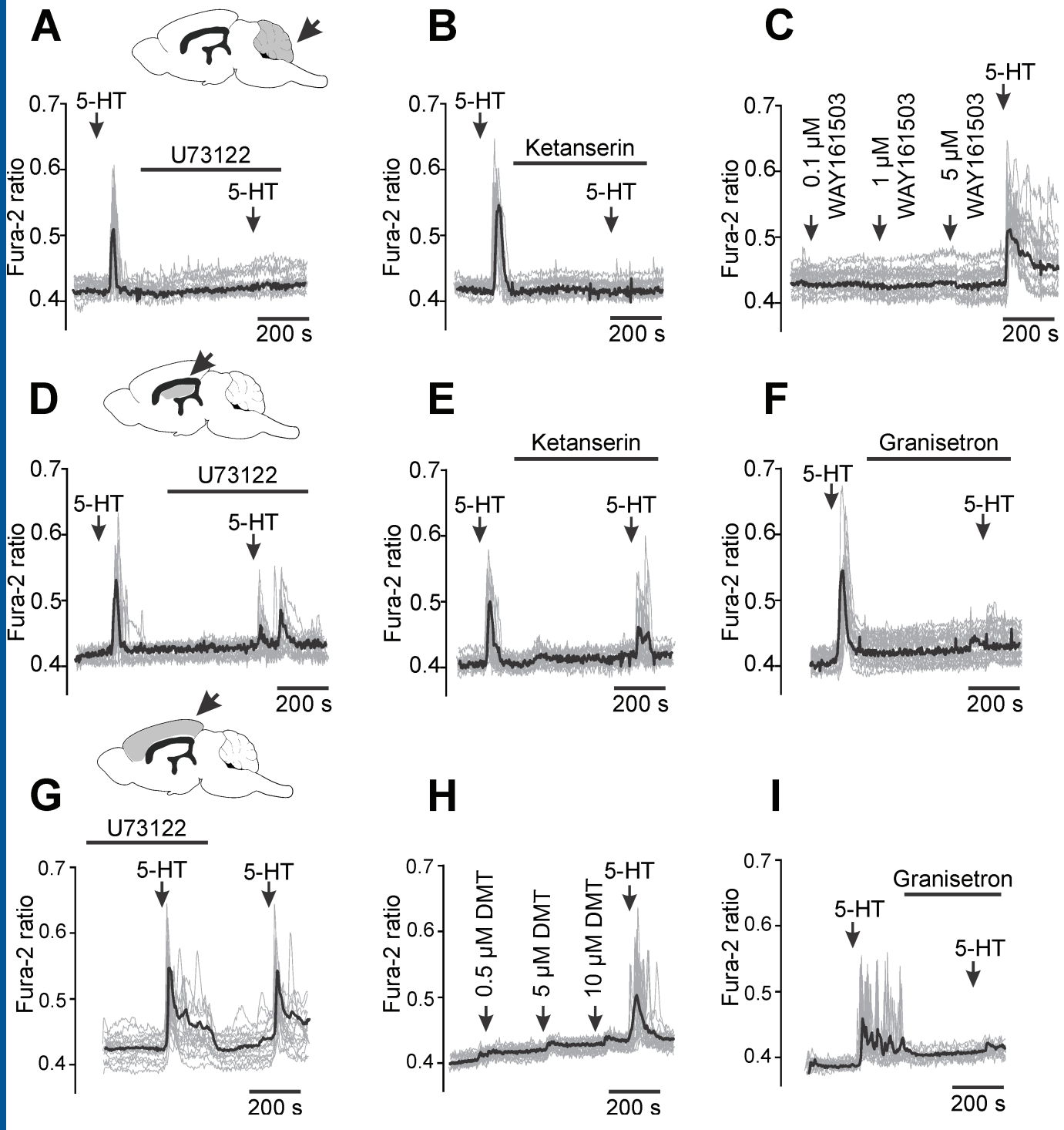

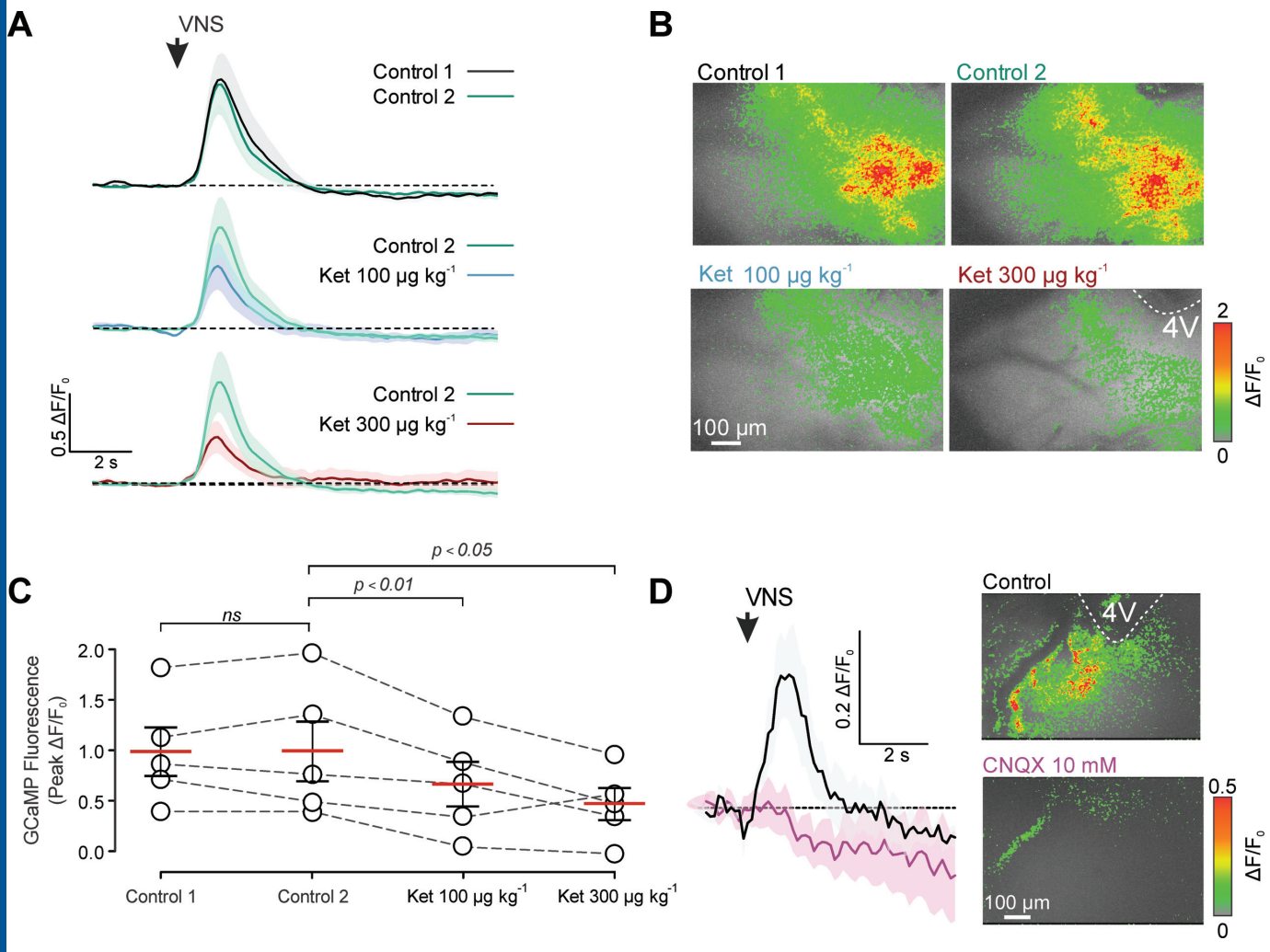

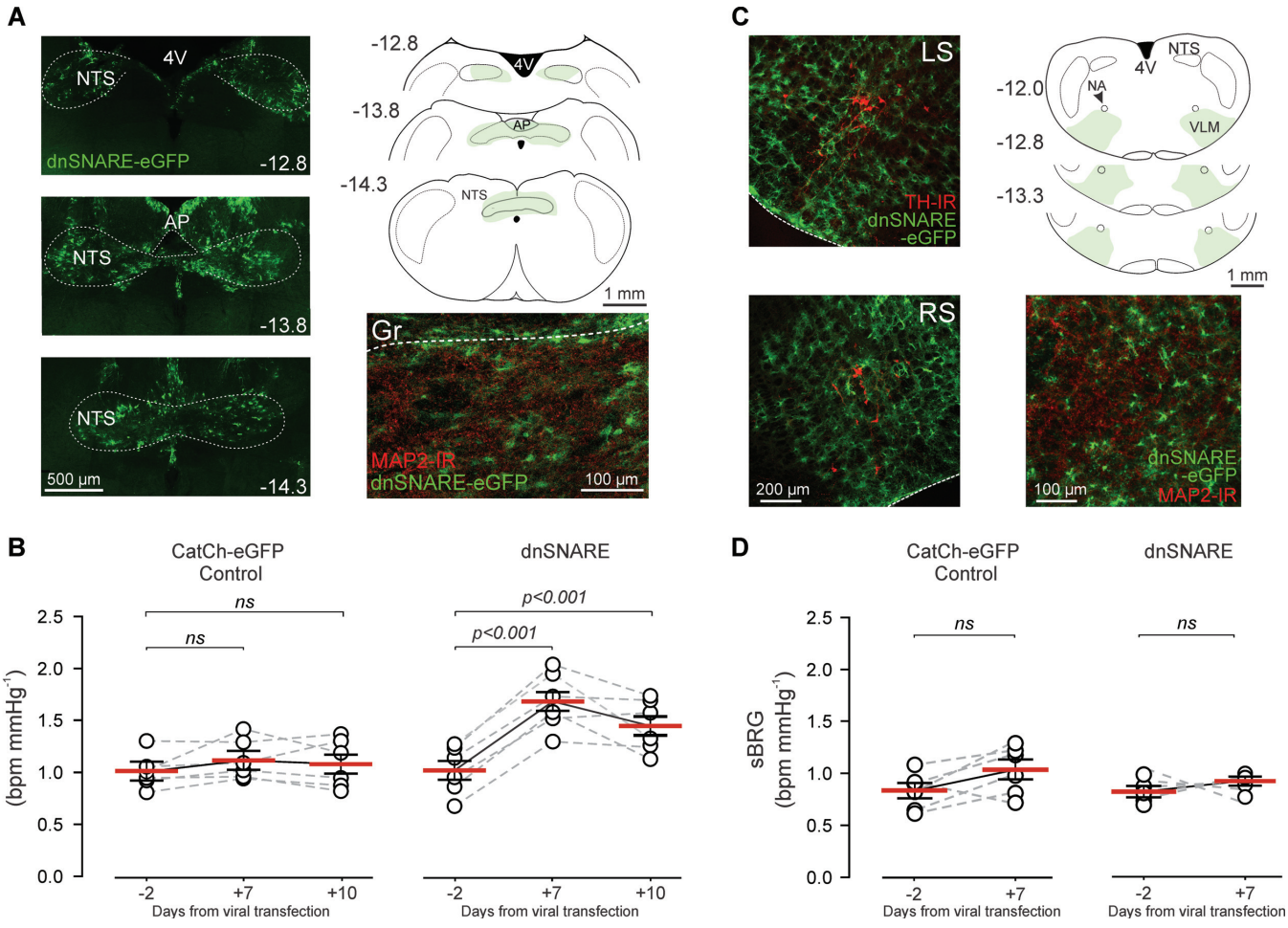

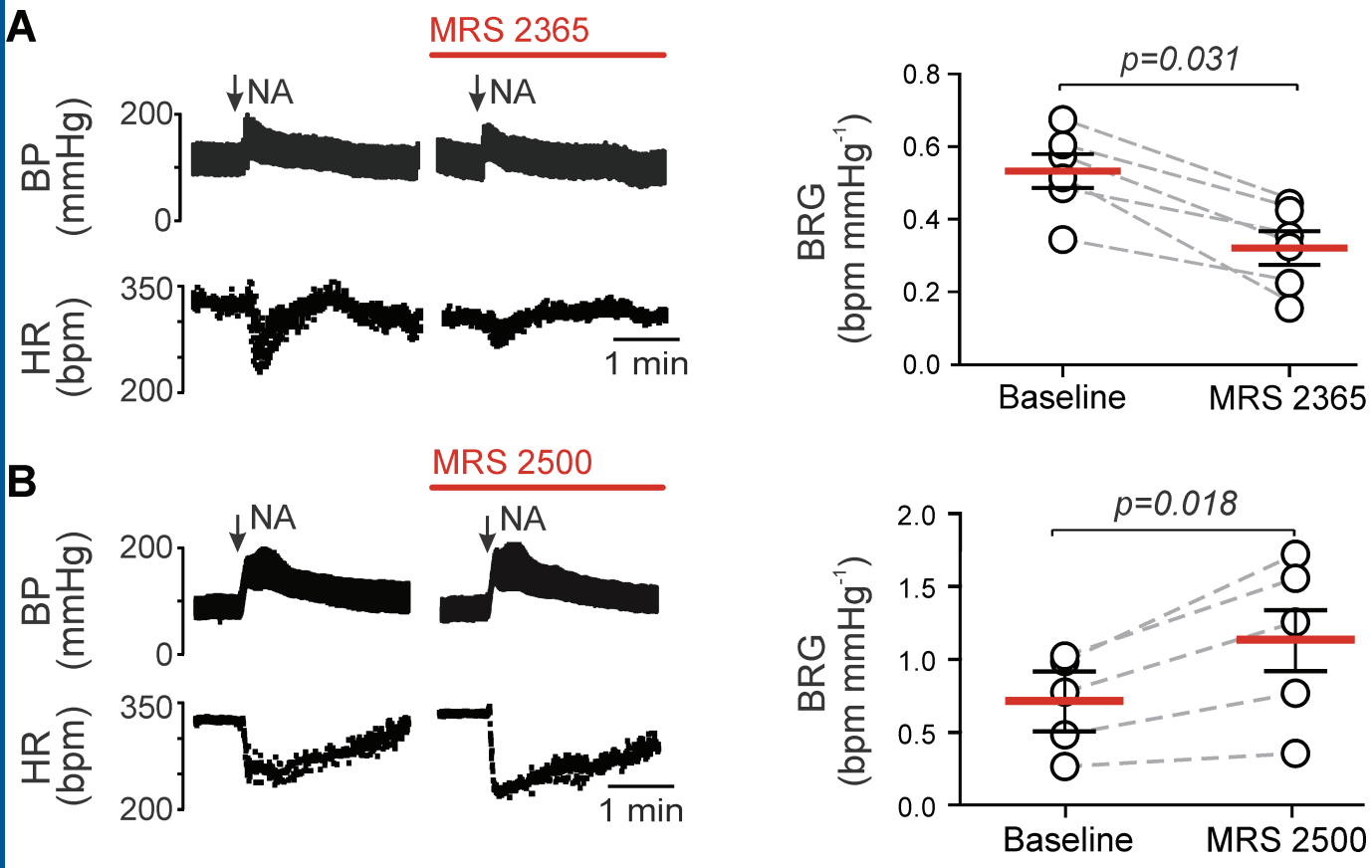

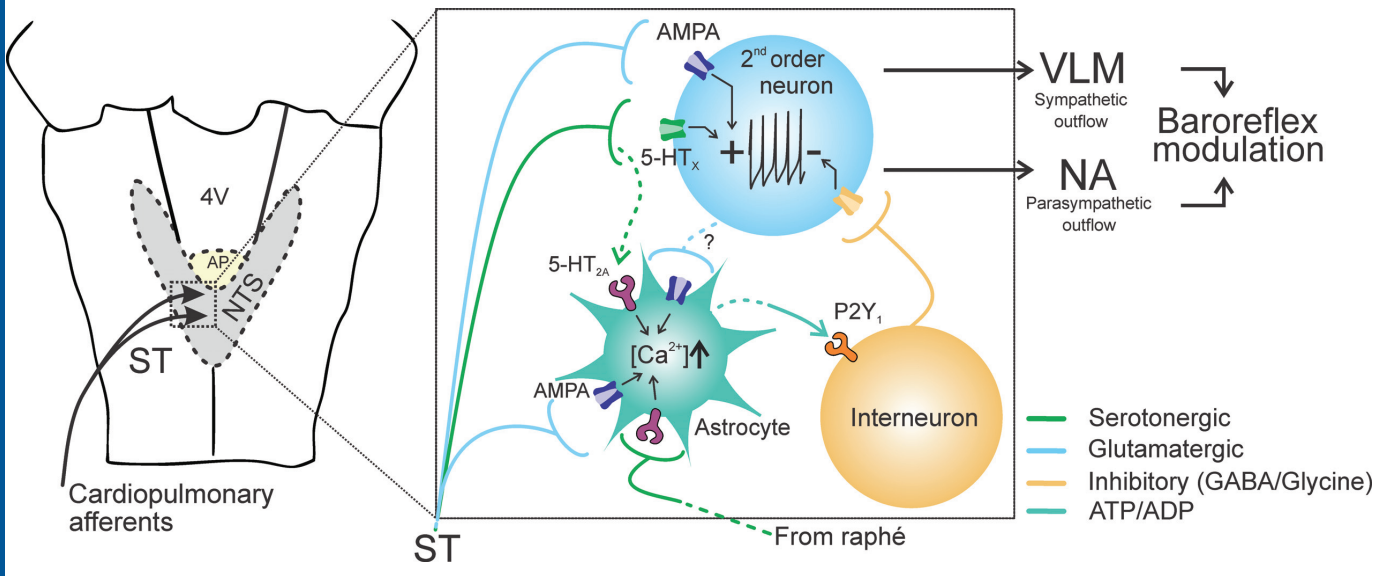

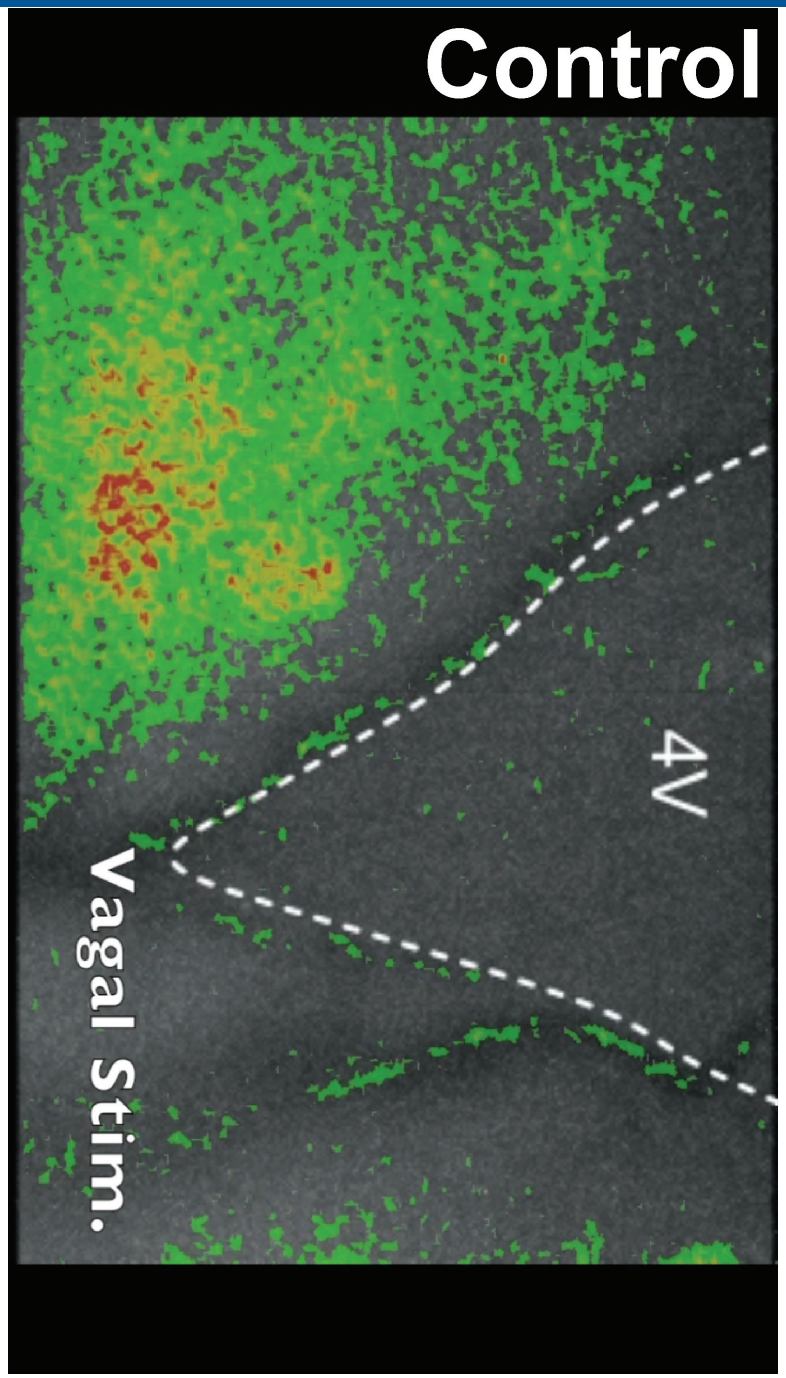

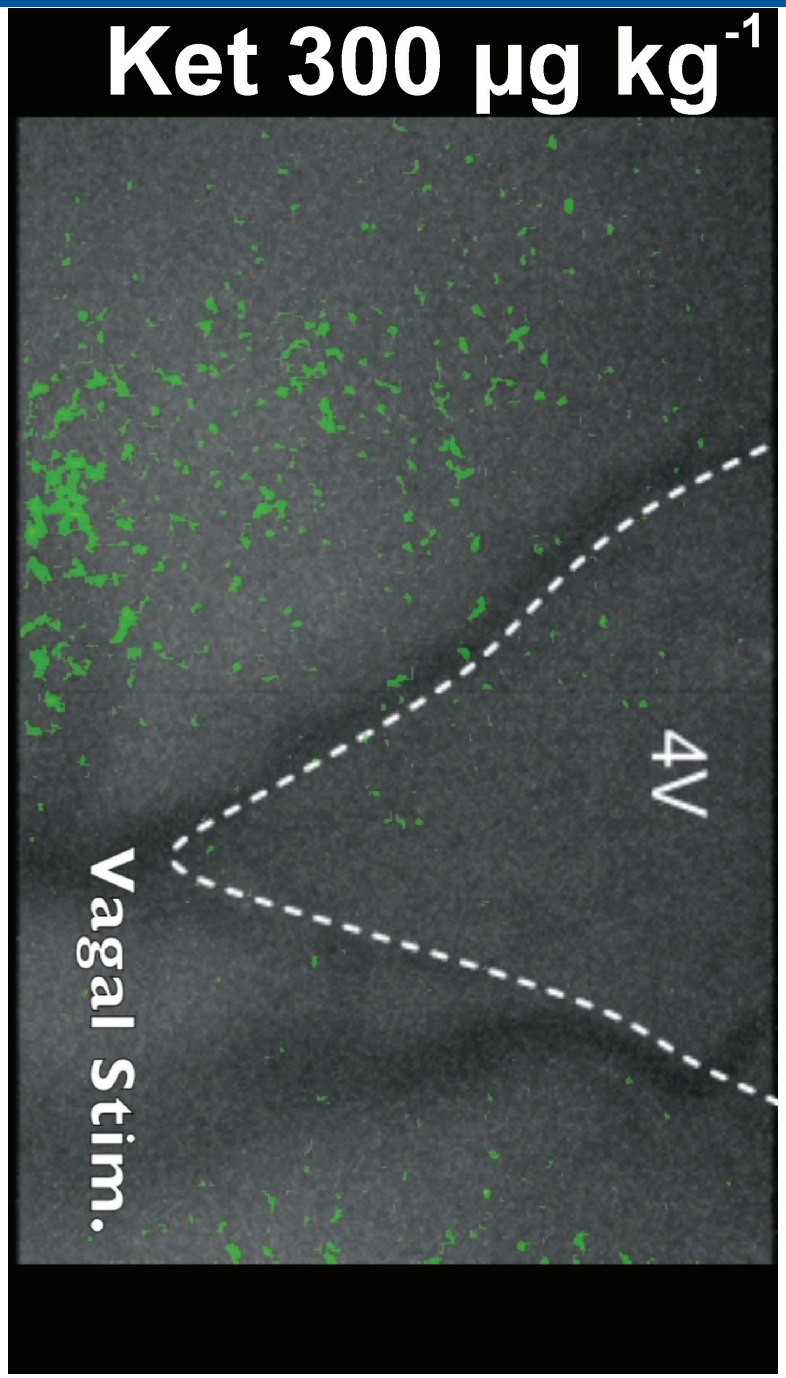
Ket 300 µg kg-1
4V
Vagal Stim.